



Article

Pressure and Liquid Distribution under the Blade of a Basket Extruder of Continuous Wet Granulation of Model Material

Roman Fekete ¹, Peter Peciar ^{1,*} , Martin Juriga ¹, Štefan Gužela ¹, Michaela Peciarová ¹, Dušan Horváth ² and Marian Peciar ¹

¹ Faculty of Mechanical Engineering, Institute of Process Engineering, Slovak University of Technology in Bratislava, Námetie Slobody 17, 812 31 Bratislava, Slovakia; roman.fekete@stuba.sk (R.F.); martin.juriga@stuba.sk (M.J.); stefan.guzela@stuba.sk (Š.G.); michaela.peciarova@stuba.sk (M.P.); marian.peciar@stuba.sk (M.P.)

² Faculty of Materials Science and Technology in Trnava, Advanced Technologies Research Institute, Slovak University of Technology in Bratislava, Ulica Jána Bottu 25, 917 24 Trnava, Slovakia; dusan_horvath@stuba.sk

* Correspondence: peter.peciar@stuba.sk

Abstract: This study explores the influence of blade design on the low-pressure extrusion process, which is relevant to techniques like spheronization. We investigate how blade geometry affects the extruded paste and final product properties. A model paste was extruded through a basket extruder with varying blade lengths to create distinct wedge gaps (20°, 26° and 32° contact angles). The theoretical analysis explored paste behavior within the gap and extrudate. A model material enabled objective comparison across blade shapes. Our findings reveal a significant impact of blade design on the pressure profile, directly influencing liquid distribution in the paste and extrudate. It also affects the required torque relative to extruder output. The findings of this study hold significant implications for continuous granulation, a technique employed in the pharmaceutical industry for producing granules with uniform size and properties. Understanding the influence of blade geometry on the extrusion process can lead to the development of optimized blade designs that enhance granulation efficiency, improve product quality, and reduce energy consumption. By tailoring blade geometry, manufacturers can achieve more consistent granule characteristics, minimize process variability, and ultimately produce pharmaceuticals with enhanced efficacy.

Keywords: extrusion; continuous granulation; particulate material formation



Citation: Fekete, R.; Peciar, P.; Juriga, M.; Gužela, Š.; Peciarová, M.; Horváth, D.; Peciar, M. Pressure and Liquid Distribution under the Blade of a Basket Extruder of Continuous Wet Granulation of Model Material. *J. Manuf. Mater. Process.* **2024**, *8*, 127. <https://doi.org/10.3390/jmmp8030127>

Academic Editor: Steven Y. Liang

Received: 26 May 2024

Revised: 13 June 2024

Accepted: 14 June 2024

Published: 18 June 2024



Copyright: © 2024 by the authors. Licensee MDPI, Basel, Switzerland. This article is an open access article distributed under the terms and conditions of the Creative Commons Attribution (CC BY) license (<https://creativecommons.org/licenses/by/4.0/>).

1. Introduction

The extrusion of powder materials as a paste is a process in which equipment based on different principles is used. It is usually a low-pressure extrusion, achieved in equipment such as a dome, radial, axial or basket extruder. These results in the final product either in cylindrical form (noodles) or in an intermediate product, which is further processed into a microgranulate by another operation, for example, in a rotating plate by spheronization [1,2].

In all these extruders, the main problem is the regulation of the extrusion pressure P . One of the possibilities is to modify the rheological properties of the paste by adding a suitable lubricant or by varying the moisture content of the paste w . However, both methods modify the character of the paste. In the case of additives, the final result manifests in the presence of substances that are unnecessary for the final product. If the rheological properties are adjusted by changing the amount of a liquid phase, other problems arise. If the amount of the liquid phase is low, extrusion pressure P rises, and the extrudate is hard, which causes a problem with its further processing into micro granules.

In contrast, the presence of a larger amount of liquid phase decreases the strength of the extrudate. The individual extrudates stick to each other and the wall of the device,

rendering the formation of micro granules impossible. In addition, any increase in the liquid content causes an increase in the financial costs associated with drying the product [3,4].

However, it is not always necessary to adjust the rheological properties of the paste in this way. An effective tool is the regulation of extrusion pressure by changing the geometry of the extrusion element: the blade (radial or basket extruder) or the end of the screw (dome or axial extruder) [1,4].

It is necessary to clarify what is meant by the term the geometry of the extrusion element. This geometry refers specifically to the angle α_i formed between the blade and the die surface. This configuration creates a wedge between the blade and the die (matrix). The movement of the blade across the die surface, combined with the adhesive characteristics of the paste, plays a crucial role in drawing the material into the narrowing wedge space. Adhesion in this context is determined by the wall friction angles between the paste and both the blade and die surfaces.

Furthermore, phenomena like liquid film formation and liquid migration are essential considerations for a complete understanding of this process. Thus, the paste is gradually pulled into the wedge gap and is compressed. This compression creates the extrusion pressure P , which increases to a value at which the paste is forced to flow through the holes of the die. Here, the extrudate is formed into the shape and dimensions of the holes in the matrix. It is the angle of the wedge gap α_i , which has a significant effect on two very important phenomena, namely the distribution of extrusion pressure in the wedge gap and the associated migration of the liquid phase in the paste before it is pushed through the holes of the matrix [5–12].

The smaller the angle of the wedge gap α_i , the greater the predominance of the normal component of the force N_i , which pushes the paste into the holes of the nozzle. Conversely, the greater this angle, the greater the effect of the shear force T_i , which forces the paste to move tangentially to the die surface. This inserts a shear stress τ_i into the paste, as a basic parameter of the rheological properties of the paste, together with the rate of shear strain $\dot{\gamma}$ of the paste [3,8,13].

The rate of shear strain $\dot{\gamma}$ of the paste affects the apparent viscosity of the paste η_z . If the moisture of the paste w is constant, the interaction of the three parameters, normal stress σ , shear stress τ and the rate of shear strain $\dot{\gamma}$, is reflected in the resulting extrusion pressure P [3,5].

However, the extrusion pressure P distribution under the blade has a complicated behavior. It can be assumed that the smallest values are on the inlet side, where the wedge gap is the widest, and the paste enters it. It is gradually compressed, which increases the extrusion pressure P , which reaches a maximum value at a certain point under the blade. This pressure profile causes the liquid in the gaps between the particles to migrate in the direction of the pressure drop, thus changing the paste homogeneity [9,11,14].

The aim of this study is to investigate the relationship between the geometry of the extrusion blade and the speed of its movement as independent parameters that influence the pressure profile in the paste in the wedge gap between the die and the blade. Then, we will examine how this pressure profile affects the migration of the liquid phase under the blade and in the extrudate [9,11,14].

To facilitate a comparative analysis of the aforementioned effect, a specific granular material is required. This material, upon the addition of a controlled amount of liquid phase, should transform into a paste with suitable rheological properties for extrusion through blades with varying geometries. However, investigating the extrusion process with specific materials often presents economic challenges due to potentially high material consumption and cost. Therefore, for investigating specific phenomena, utilizing a model material offers a more advantageous approach. This strategy was adopted in the present work. The primary component chosen was very finely ground limestone. Additionally, a specific amount of sand was incorporated to enhance the rheological properties of the paste. This combination allows for exploring the influence of various extruder blade geometries and paste moisture content on the extrusion process. [9,11,14].

2. Materials and Methods

2.1. Experimental Material

A model material was used for the experiments. It was a mixture of very finely ground limestone, sand and water. The aim of the work is not to investigate the properties of a particular material but to study the extrusion process in terms of pressure distribution under the blade and the associated accompanying phenomena when the geometry of the extrusion blade is changed.

At first, a paste made of fine-grained material with water was tested. It was very finely ground Calmit limestone from Baunit s.r.o—Rohožník, Slovakia. Due to its particle size distribution, limestone represents a wide range of powders used in the pharmaceutical, chemical, food and related industries. The physical properties of the individual components and the model material mixture are shown in Table 1. The physical properties of the individual components and the model material mixture are shown in Table 1. The physical properties were measured by standardized tests (particle shape: electron microscope JEOL IT300LV (Jeol Ltd., Welwyn Garden City, UK), particle density: helium pycnometer Quantachrome Micro Ultrapyc 1200e (Quantachrome Instruments, Inc., Boynton Beach, FL, USA), bulk density: rheometer of powder materials Freeman Technology FT4 (Freeman Technology Ltd., Tewkesbury, UK), porosity for bulk material: porosimeter Quantachrome PoreMaster-60 GT (Quantachrome Instruments, Inc., Boynton Beach, FL, USA), particle size distribution: Malvern Mastersizer 3000 (Malvern Panalytical Ltd., Malvern, UK), compressibility: uniaxial pressing on a KISTLER electromechanical press (Kistler Group, Hook, UK) with a 20 mm diameter press, strength diagram of the mixture: rheometer of powder materials Freeman Technology FT4).

Table 1. Physical properties of individual components of the 80% limestone + 20% sand model material.

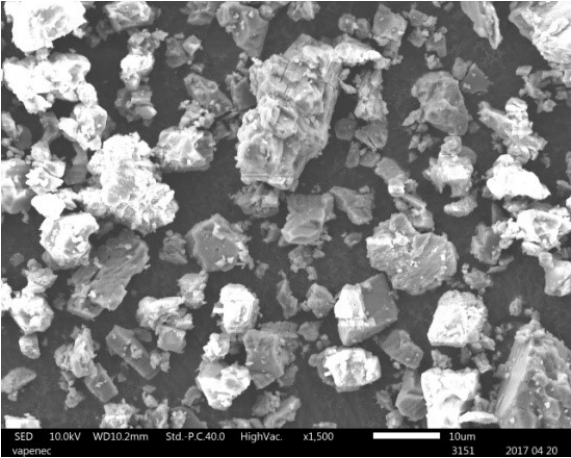
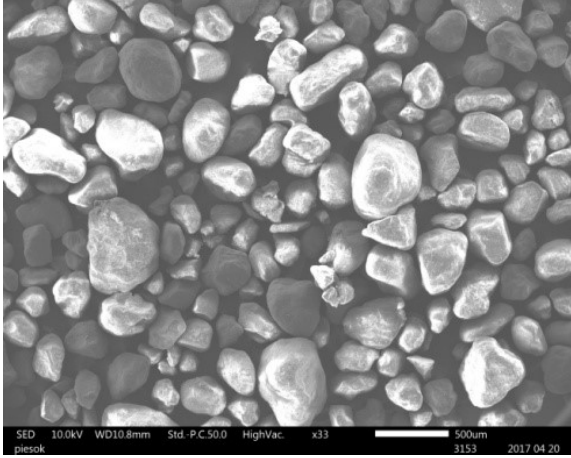
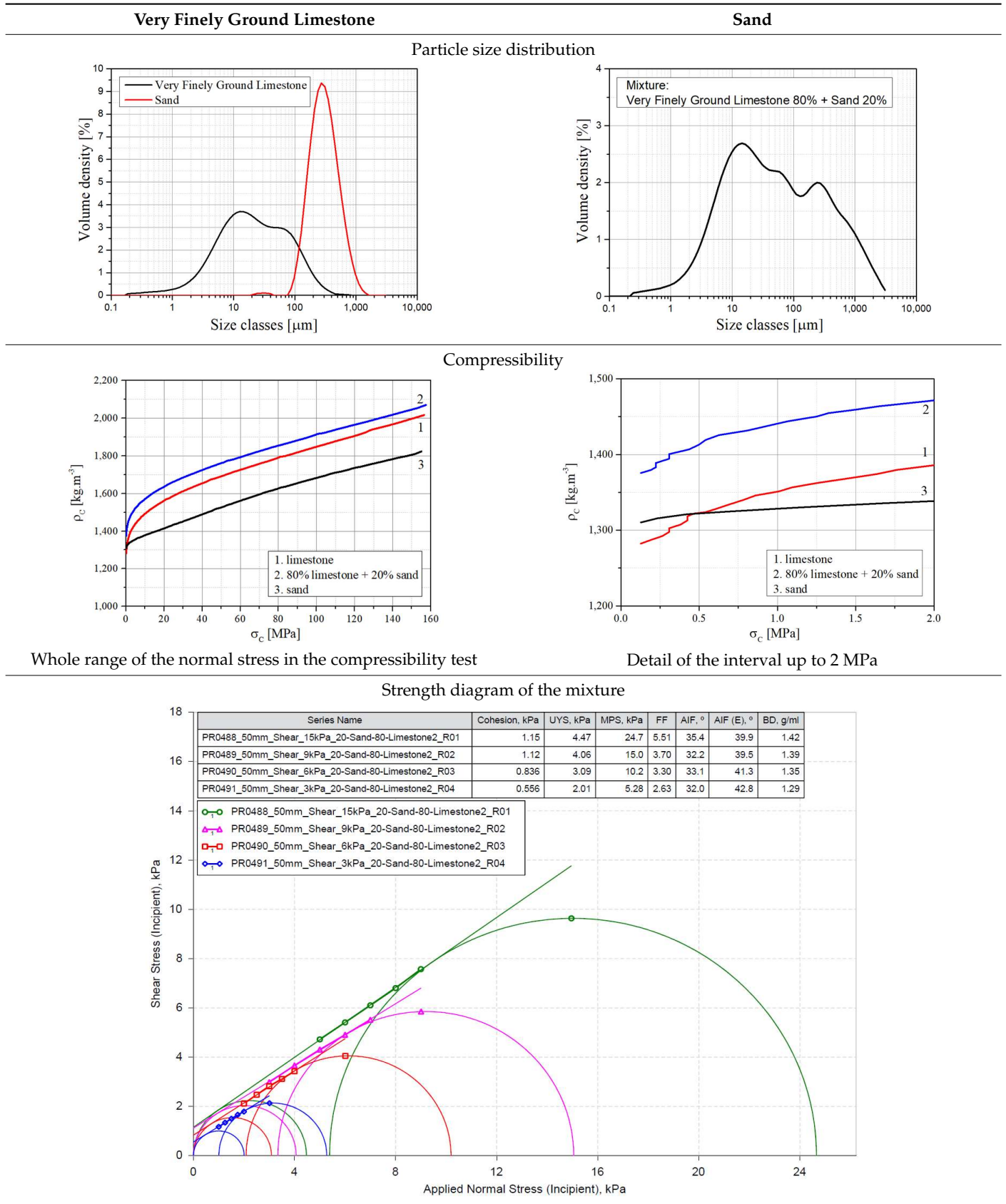
Very Finely Ground Limestone	Sand	
Particle shape		
		
$\rho_S = 2702.8 \text{ kg}\cdot\text{m}^{-3}$	Particle density	$\rho_S = 2630.5 \text{ kg}\cdot\text{m}^{-3}$
$\rho_N = 986.7 \text{ kg}\cdot\text{m}^{-3}$	Bulk density	$\rho_N = 1615.1 \text{ kg}\cdot\text{m}^{-3}$
$\varepsilon_i = 0.650$	Porosity for bulk density	$\varepsilon_i = 0.386$

Table 1. Cont.



However, one property of this limestone is that it can be processed as a paste only in a very narrow moisture range, approximately $w = 14 - 17\%$. This phenomenon is an important factor for the processes associated with the material in the pharmaceutical industry in the production of drugs by the wet method, which is why this experimental material was chosen as a model, even though limestone and sand are not directly relevant materials in the pharmaceutical industry [15–17]. At a lower moisture level, a higher extrusion pressure is required. As a result, there is a risk of the paste dewatering and stopping the extrusion. At a higher moisture level, extrusion usually occurs without major problems, but the extrudate is too wet. Then, there is a problem with maintaining its shape. In addition, if the extrusion is to be followed by spheronization, the extrudate or the microgranulate sticks together.

The same problems occur in real applications in the pharmaceutical industry, where continuous wet granulation processes such as extrusion, spheronization and continuous twin-screw granulation are applied. Regardless of whether the materials in question are genuine pharmaceutical excipients combined with Active Pharmaceutical Ingredients (APIs) or any other mixture, a rigorous two-step analysis is essential. The first step prioritizes the processing aspects and the resulting product's desired mechanical and physical properties, which aligns with the focus of this study. The second step delves into a detailed analysis of the manufactured products, encompassing various considerations such as their chemical composition, potential changes in crystallinity and polymorphism, and the influence exerted by the API content [18–21].

Bearing this comprehensive approach in mind, a model material was selected specifically to validate the first step. This material selection extends the applicability of the findings beyond the pharmaceutical industry, encompassing the chemical, agricultural, and potentially even fertilizer production sectors.

Such fine-grained material was unusable for extrusion with the geometry of some of the blades that were to be used for the experiments. Sand, with its particle shape, particle size distribution and significantly lower compressibility, is an inert material that extends the properties of the paste. This allows the paste to be examined in a wide range of tested extrusion parameters. Figure 1 shows the configuration of two separate materials of different particle size, polydispersity and compressibility.

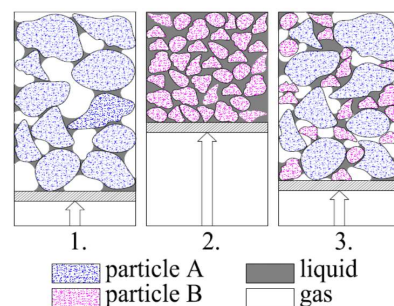


Figure 1. Configuration of the paste skeleton of different materials: (1) sand; (2) very finely ground limestone; (3) a mixture of sand and very finely ground limestone. $\epsilon_1 > \epsilon_2 < \epsilon_3$, $\Delta\epsilon_1 < \Delta\epsilon_2 > \Delta\epsilon_3$.

2.2. Influence of Normal and Shear Stresses on Extrusion Pressure

There are several principles and devices used in paste extrusion [4,22–26]. One of these principles is to extrude the paste through a perforated matrix with a blade inclined at an angle to the surface of the matrix.

In such devices, the ratio between the diameter and depth of the die hole is relatively small; often the diameter of the hole is greater than the thickness of the die. The purpose is not to form a hard cylindrical extrudate but only to preform the paste and thus obtain an extrudate suitable for spheronization, for example [3,4].

The principle of such a device is shown in (Figure 2). It is a radial or basket extruder. The blade (1), or generally the extrusion element, has such a geometry that, together with

the matrix (2), it forms a tapered wedge gap. Due to the adhesive forces, the paste (3) is drawn into the wedge gap when the inclined blade moves. Here, it is compressed, and when the optimal extrusion pressure P is achieved, the paste starts to flow through the openings of the matrix (2) [3,4].

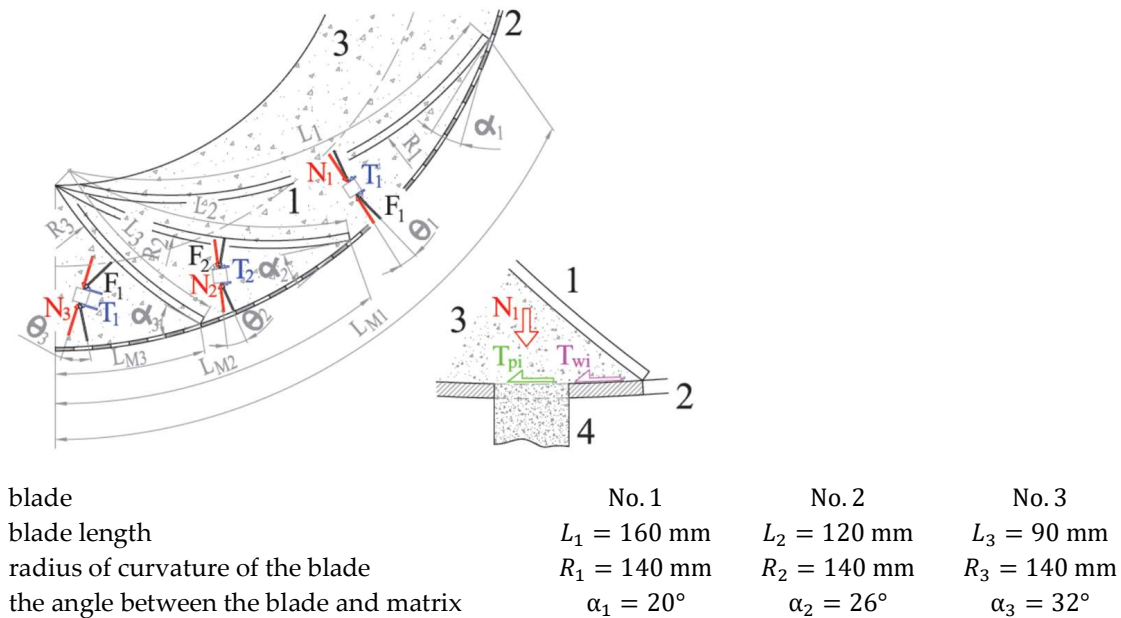


Figure 2. Radial extruder with the different geometries of the extrusion blade: (1) blade; (2) matrix; (3) paste; (4) extrudate.

The integral force F_i in Figure 2 represents the integral value of the extrusion pressure P that is distributed on the surface of the blade. If a suitably oriented control volume [3] is selected in the paste, this force can be expressed as two components. The radial component N_i is perpendicular to the surface of this volume. Its effect is manifested by compressing the paste in the wedge gap, thus creating normal stress σ_i . The tangential component T_i acts in the direction of the tangent to the surface of the control volume and creates shear stress τ_i . The index i varies according to the geometry of the blade, defined by the radius of curvature R_i and the angle α_i [3,4].

The ratio between the components N_i and T_i and the direction of action of the integral force F_i is given by the geometry of the blade. The blade can be straight or curved. It is important to define its length L_i , radius R_i and the apex angle of the wedge gap α_i . Their interactions then manifest themselves in the form of a measurable quantity, i.e., the extrusion pressure P [4,5].

In general, both the pressure p and the extrusion pressure P , are defined by the relationship between the tensors of normal and shear stresses [3,5,14,27]

$$\sigma = p\delta + \tau \tag{1}$$

where σ is the tensor of normal stresses, τ is the tensor of shear stresses, δ is the unit tensor, p is the pressure.

Due to their consistency, pastes represent a multiphase system, the basis of which is a skeleton of granular material, a solid phase. The gaps between the particles are filled with a liquid phase, which has the function of a lubricant, and its content defines the rheological properties of the paste during extrusion. Behind the matrix, in the extrudate, it forms capillary bridges, which ensure the strength and shape of the extrudate before further processing, e.g., by spheronization or drying [1,28–31].

The multiphase composition of the paste creates the preconditions for two approaches to the study of the paste extrusion process. The first is based on the mechanics of particulate

matter and considers the paste to be a discrete or semi-continuous environment. It uses experimental procedures of the mechanics of particulate matter. The second approach assumes that the paste is a continuous environment, a continuum. This approach is based on the study of its rheological properties. From the point of view of extrusion, these two principles work simultaneously. First, the granular material is compressed and consolidated in the extruder. This is followed by extrusion through the holes of the die or matrix. This is caused by the effect of a screw or blade. The structure of the grains in the skeleton is reorganized, and the distribution and size of the pores change. At the same time, the tension in the skeleton increases until the yield locus state is reached. At this moment, the granular skeleton is set in motion. However, since the liquid phase is also present, it moves in the pores between the particles. These phenomena are described by the mechanics of particulate matter and are not significantly dependent on the rheological properties of the system [1,2,9,10,22,27,32–34].

When the skeleton is consolidated, a certain degree of liquid saturation of the pores S is reached. If it is close to the value $S = 1$, the system becomes a paste, and the extrusion process is influenced by its rheological properties [4,13,33–35].

These two approaches are reflected in two important parameters of extrusion. These are the extrusion pressure profile P_i as a measurable parameter and the homogeneity of the paste from the point of view of the distribution of the liquid phase w_i . These two parameters interact with each other. This is reflected in the fact that the higher the extrusion pressure P is required, the more the fine-grained skeleton of particulate matter is compressed. However, the more it is compressed the more inhomogeneity of the pore distribution among the particles is presented. This results in fluid migration towards to larger pores. The distribution of the liquid in the pores, as a basic parameter of the rheological properties of the paste, affects the extrusion pressure P . Thus, the extrusion process is stabilized when the balance between the extrusion pressure profile P_i and the liquid distribution w_i in the pores of the skeleton of the particulate matter is set [4].

Applying these notes on the process to the basket extruder with different blade geometries, it is possible to compile a diagram of the interactions that occur during extrusion (Figure 3).

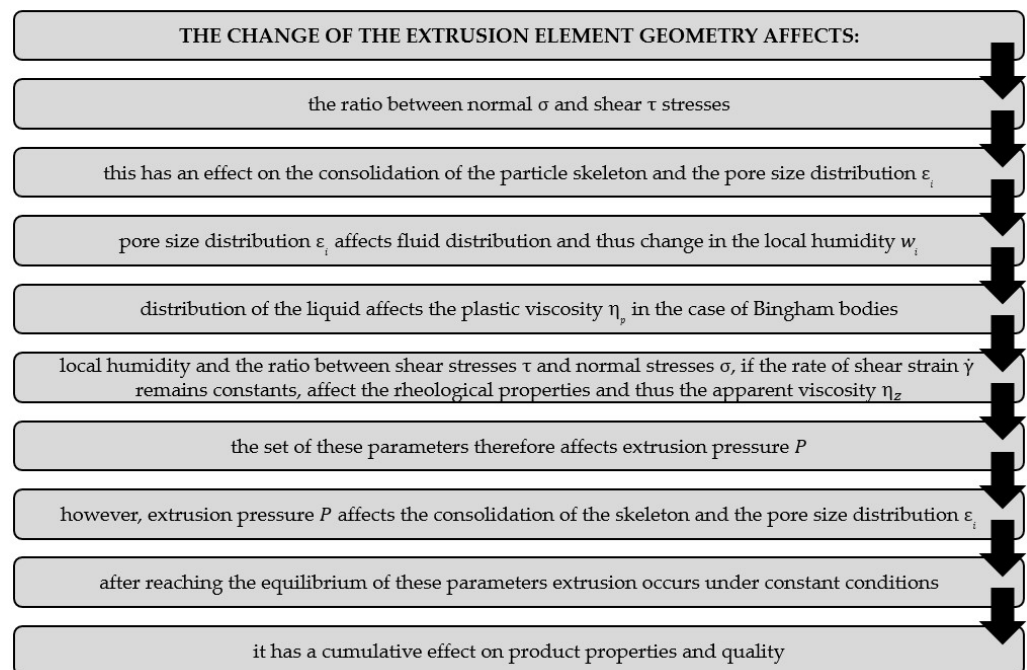


Figure 3. Scheme of influences of extrusion parameters.

The consolidation of the particulate material is one of its basic states, which is obtained under the influence of the pressure P_{cons} , which is a directly measurable parameter. However, it must be said that it acquires its under-consolidated, consolidated or over-consolidated state by the interaction of normal stresses σ and shear stresses τ . The normal stress σ compresses the granular material, and due to the mutual contact of the particles, a shear stress τ is generated among them. If the equilibrium is disturbed, the grains are moved to a new, more stable position. It results in a reduction of the volume of the gaps between the particles. If there is liquid in the gaps, the saturation S will increase. The stress state, defined in this way, is interesting, especially until the moment when the flow occurs. In the mechanics of particulate materials, it is a state when the stresses are on the yield locus [2,32,35,36]. The granular skeleton comes into motion, and flow occurs [37,38]. The strength diagram of the particulate material describes the different states of consolidation. Each of them corresponds to one locus yield. It follows that a certain locus yield corresponds to a specific consolidation, which is achieved for only one pressure P_i . For each consolidation, only one density of the paste, or wet particulate material, ρ_{pi} is also achieved.

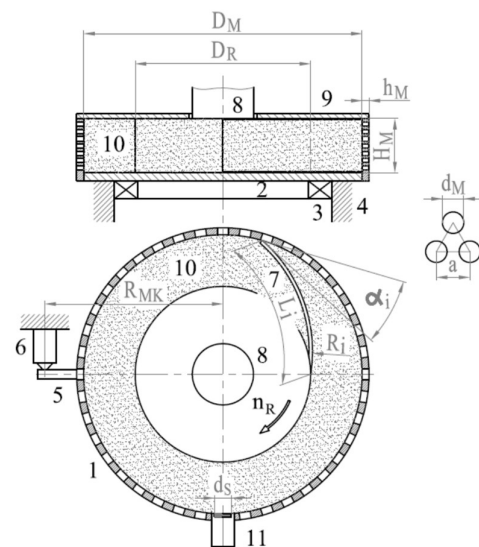
It follows from this note that for the testing of the extrusion of pastes, the primary effect is the extrusion pressure P . Then, the wet particulate material can be considered as a quasi-continuous medium, i.e., a paste. The influence of the consolidation of the skeleton formed by the particulate substance is also manifested. Its consolidation is defined by the voidage or porosity ε_i . This parameter, together with the liquid content, indicates the degree of saturation of the pores by the liquid S [15].

Ultimately, the course of the extrusion pressure P in the wedge gap is reflected in two facts. It is the migration of the liquid phase in the opposite direction to that of the increase in pressure P . The second manifestation is the amount of extrudate m_{ei} behind the matrix, varying along the narrowing wedge gap [15].

In the next part of the text, attention is paid to the extrusion process in terms of pressure distribution P_i under the extruder blade, liquid migration in the granular skeleton w_i due to inhomogeneity of pore distribution ε_i and the moisture distribution w_{ei} in the extrudate just behind the matrix. In addition, the dependence of the mass flow m_{tei} of the wet material through the holes in the matrix as a function of the pressure profile of the extrusion pressure P_i under the blade is investigated [15–17].

2.3. Experimental Equipment

The experiments were performed in an extruder with a cylindrical perforated matrix (Figure 4). The edge of the extrusion blade moved over the surface of the matrix. The device consists of a matrix (1) which is mounted on a plate (2). The plate (2) is on a bearing (3), which is connected to the frame (4). An arm (5) of the plate (2) is supported by a force sensor (6). This configuration allows the measurement of the torque M_{ki} as the result of the shear component T_i of the integral force F_i . For each series of experiments, the configuration with only one blade (7) was used. This blade was placed on a rotor (8), which is driven by a motor gearbox. It allows various speeds n_R to be set. A lid (9) is placed on top of the matrix (1), thus creating a closed chamber in which the paste (10) is located. The matrix (1) is made of a perforated metal sheet of thickness h_M and rolled into a cylindrical shape. The diameters of the holes in the matrix are d_M with distance a , and the holes are in a triangular configuration. A jig for the location of the pressure sensor (11) is welded on the outer side of the matrix. This sensor has a ceramic membrane of 18 mm diameter. It was used to measure the pressure P .



inner diameter of the matrix	$D_M = 255 \text{ mm}$
matrix thickness	$h_M = 3 \text{ mm}$
thickness of the matrix	$H_M = 60 \text{ mm}$
diameter of holes	$d_M = 8 \text{ mm}$
hole spacing	$a = 12 \text{ mm}$
rotor diameter	$D_R = 160 \text{ mm}$
rotor speed	$n_R = 0 - 25 \text{ min}^{-1}$
arm of force for torque calculation	$R_{MK} = 225 \text{ mm}$
ceramic membrane diameter of the pressure transducer	$d_s = 18 \text{ mm}$

Figure 4. Laboratory radial extruder. Main parameters of the extruder: (1) matrix; (2) base plate; (3) bearing; (4) frame; (5) arm; (6) force sensor; (7) blade; (8) rotor with shaft; (9) lid; (10) paste; and (11) pressure sensor.

2.4. Experimental Measurements

The experiments were focused on the following basic areas:

- The pressure profile in the paste in the wedge gap;
- Migration of the liquid phase in the paste in the wedge gap;
- The course of the amount of extruded material through the die and its moisture depending on the extrusion pressure.

The composition of the model material (Table 1) was constant. The model material, the paste, consists of three components. For each experiment, the 4.0 kg of dry, very finely ground limestone and 1.0 kg of sand were mixed. To this mixture, 988.2 g of water was added. The dry components of the mixture were poured into the horizontal homogenizer with slow-moving blades and mixed together. Then, the water was gradually added by spraying it through the nozzle. The ratio between the solid and added liquid phase represents the absolute humidity $w = 16.5\%$.

This model material makes it possible to investigate the extrusion process at a relatively wide range of apex angles α_i , while the ratio of the thickness of the matrix h_M to the diameter of the holes d_M remains the same, without the need to change the moisture of the paste w .

The actual moisture values of the paste after homogenization varied slightly. This was due to the fact that part of the injected water remained on the wall of the homogenizer or was in the layer that was stuck to the surface, blades and shaft of the homogenizer. For this reason, each experiment is unique, and the result of the monitored parameter is the average of five measurements.

The independent variable parameters were the rotor speed n_R with the blade, the blade length L_i and the apex angle α_i .

The tested variables were the course of the extrusion pressure distribution P under the blade, the moisture distribution of the paste in front of the matrix w_i and behind the matrix w_{ei} , corresponding to the value of pressure P_i and the amount of extrudate m_{ei} . The values with the index i refer to the values obtained from the control volumes V_{ini} and V_{exi} (Figure 5e). The five control volumes V_{ini} were defined in the space between the blade and the paste matrix. The additional control volumes V_{exi} were defined for the extrudate. Their number depends on the geometry of the blade. They are defined as the radial projection of the blade length onto the matrix surface. The height of the control volume is H_M , which is the height of the matrix.

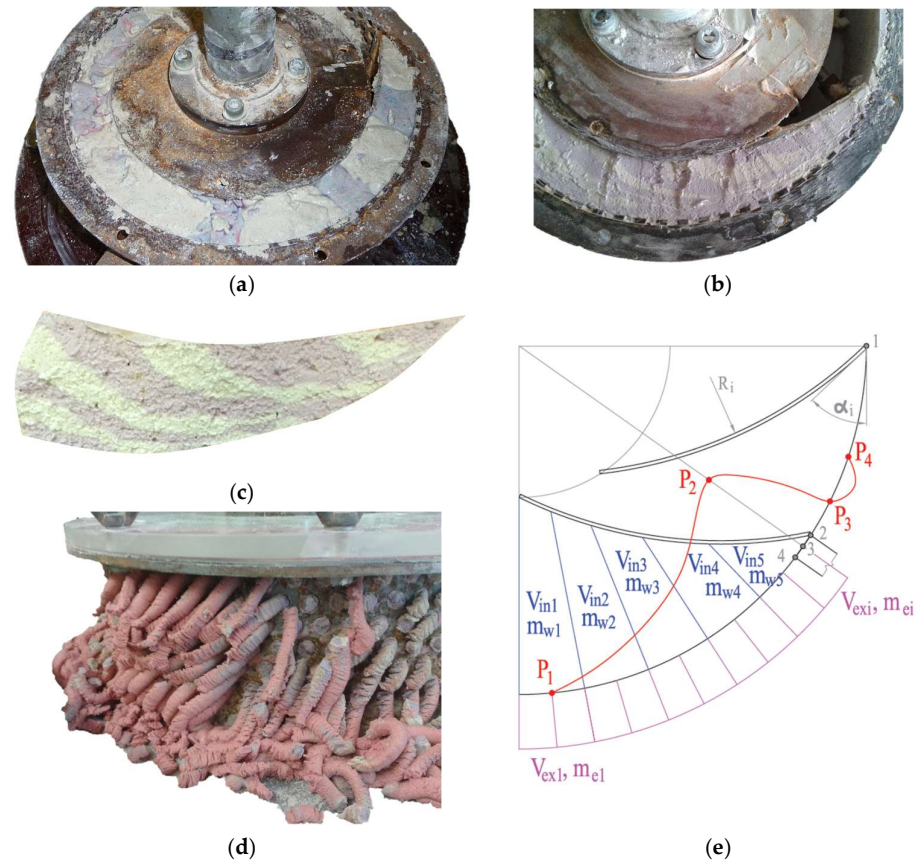


Figure 5. The main experimental steps and the definition of control volumes and pressure profile under the blade as a function of the blade position: (a) the extruder chamber filled with colored layers of paste before the experiment; (b) colored streams of the paste in the wedge after the experiment; (c) the wedge of paste from the chamber before cutting; (d) extrudate behind the matrix; (e) definition of control volumes.

After each test, a wedge of paste was removed from the space under the blade and cut into five sections defining a control volume of V_{ini} (Figure 5c). Similarly, the extrudate corresponds to the control volume of V_{exi} behind the matrix was collected (Figure 5d).

In order to monitor the flow of the paste in the wedge gap, it was necessary to color part of it. Therefore, after homogenization, it was divided into two parts. One was stained with pigment (purple tint), and the other one remained uncolored (grey tint). Each section was homogenized once more. Then, the extruder chamber was alternately filled so that the color shades alternated in the tangential direction (Figure 5a). The color differentiation made it possible to monitor the flow of the paste in the wedge gap. The paste flow monitoring experiment was performed only for rotor speed $n_R = 10 \text{ min}^{-1}$.

2.4.1. Pressure Profile in the Wedge Gap

A paste without staining was used for measuring the pressure profile in the wedge gap and for monitoring the migration of the liquid phase. Prior to each experiment, the rotor (8) with the blade (7) was positioned relative to the sensor (11) on the die (1) such that there was an angle of about 90° between the attachment point of the blade and the axis of the sensor (Figure 3). In such a position, the extruder chamber was filled with the paste (Figure 5a) and closed with a lid (Figure 3). The required rotor speed n_R was set, the measuring system was switched on, and the device was started. The rotor with the blade made one turn, and the device was turned off. A signal from the pressure sensor was recorded. The signal acquisition frequency was 10 Hz. The pressure sensor detected a pressure profile in the paste as the blade passed in front of the sensor. In this way, it was possible to obtain a pressure profile as a function of the position of the control volume under the blade.

Only the data obtained between the two blade positions were used to evaluate the experiment. The beginning is when the attachment point of the blade has reached the sensor level. This corresponds to the position of the blade edge in position 1 (Figure 5e). The interval ends when the blade edge passes behind the pressure sensor, position 4. It is assumed that the flow and pressure ratios in the wedge gap have stabilized at this, and the pressure sensor records the pressure profile under the blade as a function of blade geometry.

2.4.2. Migration of the Liquid Phase in the Paste in the Wedge Gap

This phenomenon was investigated by the mass balance of paste and extrudate in control volumes. The moisture distribution of the paste w_i in the wedge gap between the blade and the matrix was monitored by means of control volumes V_{ini} .

The moisture balance w_i in the control volumes were ascertained by weighing the mass m_{wi} of these volumes in the wet state. Then, they were dried in a chamber drying oven at a temperature of 105°C for 24 h and weighed again to get the dry weight m_{si} . The difference in weights provided the necessary data for the moisture balance and distribution w_i in the wedge gap in relation to the extrusion pressure P_i .

2.4.3. Course of the Amount of Extruded Material through the Die Depending on the Extrusion Pressure

The moisture distribution of the extrudate behind the die was evaluated by its weight in V_{exi} control volumes. The external volumes V_{exi} were also used for measuring the throughput of the extruder. It was the amount of extruded material m_{ei} measured over the individual surface areas of the matrix that correspond to external control volumes V_{exi} . These data allow analysis of the effect of pressure on the amount of extruded material.

This was repeated for every revolution of the rotor $n_R = 10/13/16/19/22 \text{ min}^{-1}$. Each experiment was carried out five times.

3. Results and Discussion

It can be seen (Figure 5c) that the paste is deformed in a tangential direction to the surface of the matrix and the blade. Layers that are closer to the matrix surface are stretched and tapered. This is due to the flow of paste towards the holes in the matrix and under the influence of the shear stresses in the paste. The layers of paste by the blade are moved in front of the blade (tangential motion) and gradually fill the free space left by the paste, which has already flowed through the holes of the matrix (radial motion). From the point of view of the rheology, it can be seen that the deformation of the paste increases from the blade towards the surface of the matrix. However, the circumferential speed also increases in this direction as a function of the radius. This means that the rate of shear strain $\dot{\gamma}$ also increases. Therefore, it is possible to assume a change in the apparent viscosity η_z in this direction. However, this is a complex phenomenon, and it would require a separate investigation, which is not the subject of this article.

3.1. Pressure Profile in the Wedge Gap

The pressure profile under the blade was recorded as a function of the position of the blade edge from position 1 to position 4, relative to the sensor axis (Figure 5e).

This figure shows a schematic principle of measurement. The positions of the blade and the sensor and the course of the measured quantities in relation to the control elements are monitored. Thus, the values of the pressure P_i and the amount of material extruded into the control elements V_{exi} are measured. The pressure profile is shown as a function of time, i.e., the time of transition of the blade above the sensor from position 1 to position 4. This time depends on the rotor speed n_R and the blade length L_i , i.e., on the geometry of the blade. At position 1, extrusion pressure P_1 begins to increase. It corresponds to the value of P_1 at the entrance to the tapered wedge gap and the extruded amount of extrudate m_{e1} . The blade moves around from point 1 to point 4. The pressure P_i increases, and the amount of extruded material m_{ei} increases in all the individual control elements. The pressure rises and reaches the maximum P_2 value when the blade is in position 2. Then, the entire sensor membrane is still under paste pressure. As the blade moves to position 3, a pressure drop is recorded. It is caused by the fact that the surface of the membrane is no longer fully loaded. The pressure acts on an ever smaller area of the membrane and therefore the P_4 pressure drops to zero at point 4. The pressure drop between points 3 and 4 to a negative value is due to the response of the unloaded membrane. The pressure values between points 2 and 4 are not considered in the results. Therefore, point 2 is considered the end of the measurement of the pressure P_i and also the amount of extruded material m_{ei} .

The results from the pressure profiles P_i and the amount of the extrudate m_{ei} were evaluated not on the length of the blade L_i but on its projection L_{Mi} on the surface of the matrix. This is because the pressure sensor is located on the matrix, and the extrudate is located behind the matrix.

Figure 6a shows the course of the extrusion pressure P as it was recorded by the pressure sensor during the motion of the blade, as can be seen in Figure 5e. According to the speed of the rotor n_R , i.e., the circumferential speed of the blade edge at the point of contact with the matrix surface, the length of the pressure profile interval also changes. Such a presentation of the pressure profile P is not advantageous. Therefore, the time interval Δt is recalculated to the projection length of the blade L_{Mi} on the surface of the matrix in relation to the circumferential speed.

After the experiment, the extruded material is located in the control elements V_{exi} (Figure 7). There is the smallest amount of this material in the control volume V_{ex1} and its properties correspond to the pressure P_1 . The weight of the extruded material m_{ei} increases from V_{ex1} to V_{ex5} . This is due to the fact that each control volume V_{exi} contains all the material from the previous elements and the material also extruded into this volume V_{exi} , which is the weight m_{ei} .

Thus, in each control volume V_{exi} , there is an extrudate whose moisture is w_i and consolidation determined by the pressure P_i , but also the extrudate with the properties from the previous control volumes. It means control volume V_{ex1} contains the material with the properties corresponding to the pressure P_1 . In control volume V_{ex2} the properties of the paste correspond to the pressure P_2 but there is also the extrudate from the previous control volume V_{ex1} . In control volume V_{ex3} , there is the paste extruded by the pressure P_3 with the corresponding properties, but also the extrudate from control volumes V_{ex1} and V_{ex2} , etc. The last control volume V_{ex5} contains the paste from all volumes. This is also the reason why control volume V_{ex1} has the least extrudate and its amount increases towards control volume V_{ex5} . It is the result of the differential weight gain in the individual volumes. The result is an inhomogeneity of the extrudate.

From a practical point of view, it is more advantageous to present the measured data not as a function of time (Figure 6a) but in relation to the projection length of the blade L_i on the inner surface of the matrix L_{Mi} (Figure 1).

Therefore, the value of time Δt on the x -axis is converted to the projection length of the blade L_{Mi} on the graphs. They are shown in (Figure 6b). They show the values of the

pressure increase P_i between points 1 to 2 (Figure 7). The pressure profile consolidates the paste and causes its extrusion.

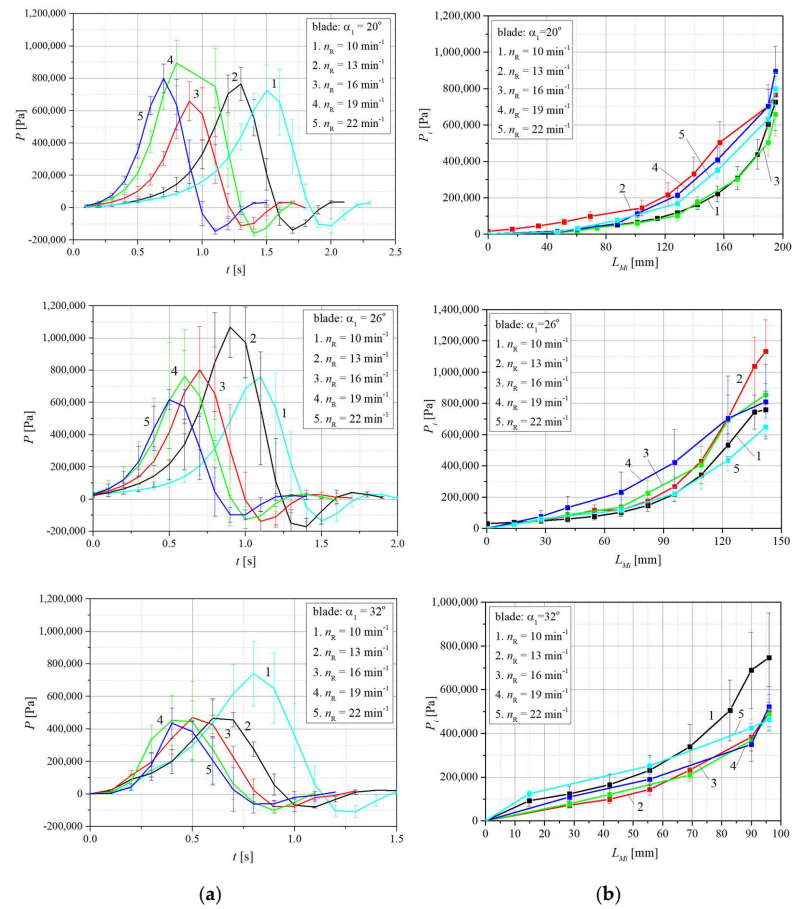


Figure 6. The pressure profiles in the wedge during extrusion: (a) before the conversion as the graphical record of the sensor; (b) after the time interval Δt conversion to the projection length of the blade L_{Mi} .

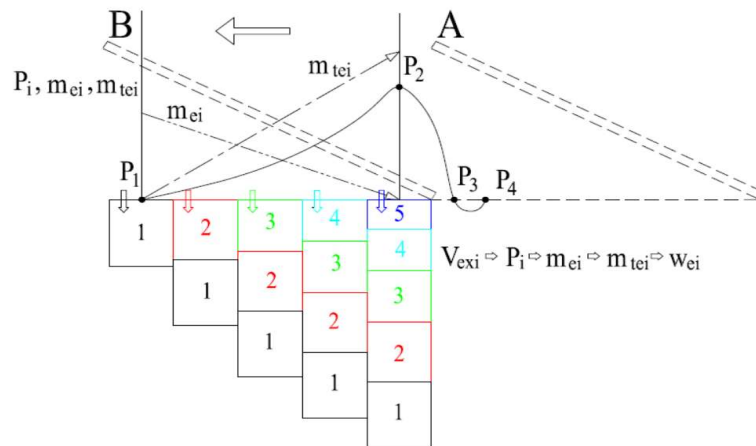


Figure 7. The process of the paste extrusion. The distribution of the extrusion pressure under the blade and the diagram of the principle of extrudate formation depending on the position of the blade, the weight of the extrudate m_{ei} and the mass flow m_{tei} .

3.2. Migration of the Liquid Phase in the Paste in the Wedge Gap

The wedge of paste was removed from the volume under the blade (Figure 5c). Then it was cut into the five control volumes of V_{in1} to V_{in5} . Each of them was weighed and then dried. After drying, it was weighed again, and a simple moisture balance was made. Each experiment was repeated five times. The results are shown in the graphs in Figure 8.

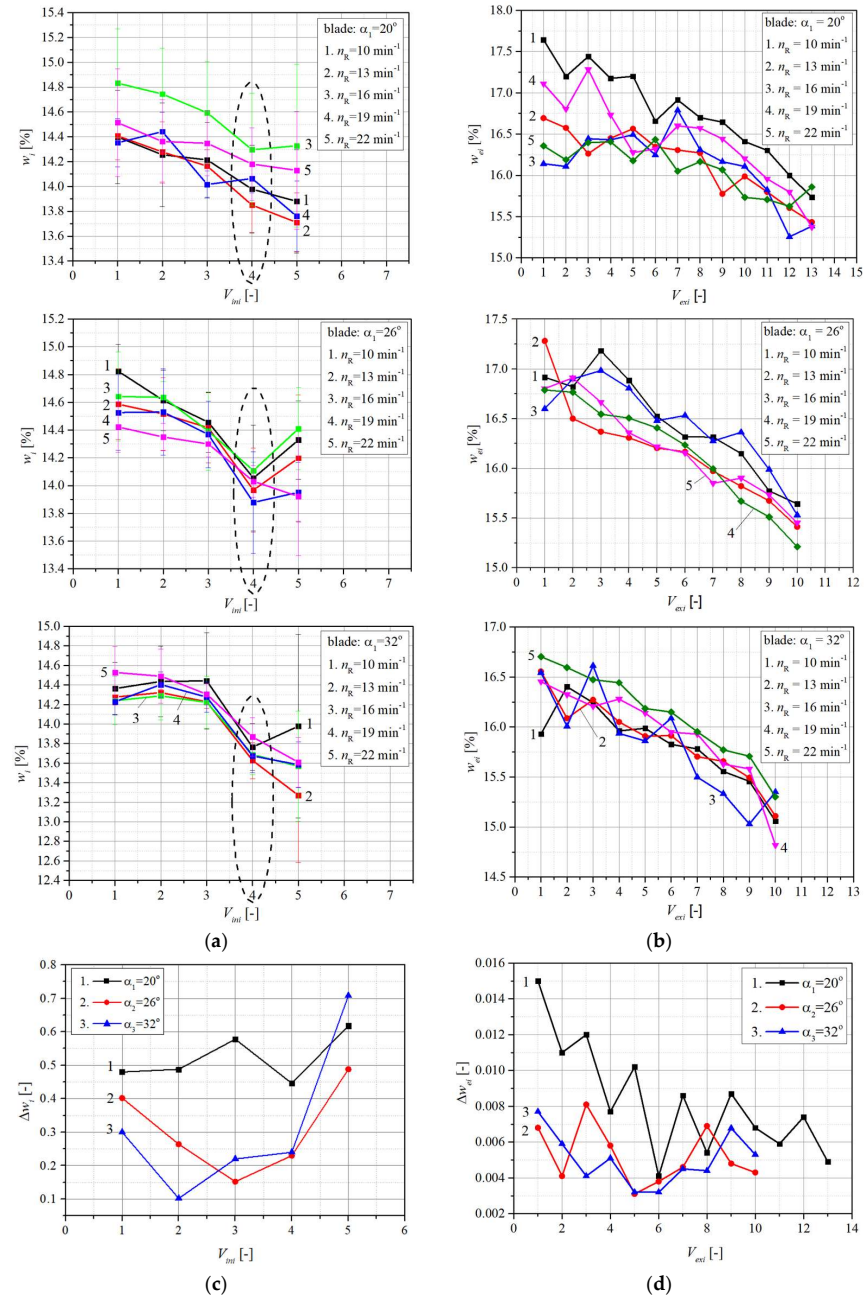


Figure 8. Comparing the liquid distribution: (a) in the wedge gap between the blade and the matrix; (b) in the extrudate; (c) interval of scattering of the average values of the moisture in the wedge gap for all speeds of the rotor; (d) interval of scattering of the average values of the moisture in the extrudate for all speeds of the rotor.

The results show that by increasing the blade inclination angle, the average moisture scatter interval for each rotor speed narrows. This fact is probably related to the rheological properties of the paste. At the 20° angle of inclination of the blade, the compression of the paste in the space between the blade and the matrix caused the normal forces to be

more pronounced than the effect of shear forces. As the angle of inclination of the blade increases, this scattering decreases, and the smallest average values are at the angle of 32° (Figure 1). At this angle, the magnitude of the normal forces is smallest, and the effect of shear forces increases. Another interesting phenomenon is the decrease of the moisture in the 4th control volume (Figure 8a), marked zone. This phenomenon would need a more detailed examination.

3.3. Amount of Extruded Material through the Die and the Liquid Distribution

The moisture of the extrudate w_{ei} decreases in the direction of the narrowing wedge gap, i.e., in the direction of the increase of the extrusion pressure (Figure 8b). This phenomenon is again related to the redistribution of the liquid inside the extruder, between the blade and the matrix (Figure 8a).

The influence of the rotor speed can be predicted as follows from the achieved results. If only the extreme speed values are taken for comparison, i.e., $n_R = 10 \text{ min}^{-1}$ and $n_R = 22 \text{ min}^{-1}$, then the following can be stated. For the angle $\alpha_i = 20^\circ$ it can be stated that the scatter w_{ei} is the largest as a function of rotor speed n_R . It is evident that at the speed $n_R = 10 \text{ min}^{-1}$ the moisture of the extrudate w_{ei} is the highest, the lowest is at $n_R = 22 \text{ min}^{-1}$. This scattering decreases towards the angle $\alpha_i = 32^\circ$. In this case, the moisture of the extrudate is highest at $n_R = 22 \text{ min}^{-1}$ and lowest at $n_R = 10 \text{ min}^{-1}$. It is important that as the angle of the blade α_i increases, the moisture of the extrudate w_{ei} decreases. This is due to the fact that the paste is less compressed and thus the migration of liquid through the holes of the matrix is less.

Figure 9a shows the course of the amount of extruded paste behind the die. For the blade with the angle $\alpha_i = 20^\circ$, which is the longest, the samples were taken from 13 control volumes of V_{exi} . For blades with angles $\alpha_i = 26^\circ$ and $\alpha_i = 32^\circ$, ten control volumes V_{exi} were provided. From these results, it is difficult to assess the effect of rotor speed with the blade on the amount of extruded material. However, it can be seen that the larger the angle, the greater the variance of the values. This is the absolute amount of extruded material, not the throughput dependent on the rotor speed. Figure 9b indirectly shows the throughput of the paste through the holes in the individual control volumes. The flow speed is hidden in the throughput of the extruder, i.e., the weight of the paste extruded through the holes of the matrix in control volumes per unit time. In this case, the effect of increasing the speed on the flow rate of the paste is evident. The throughput of the extruder increases with increasing blade angle α_i and with increasing speed n_R .

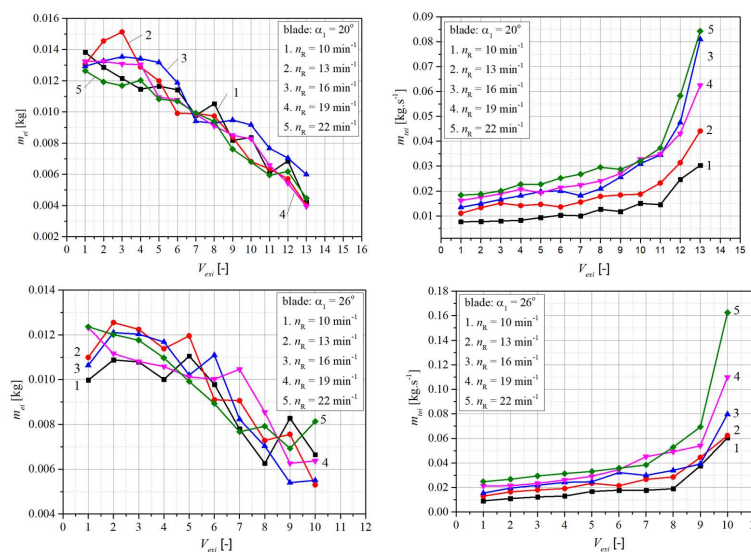


Figure 9. Cont.

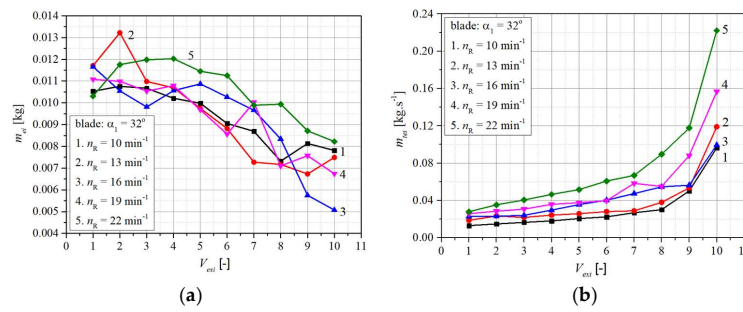


Figure 9. Balance of extruded paste in the control volumes outside the matrix: (a) weight in individual control volumes V_{exi} ; (b) weight of paste extruded through the die holes in control volumes V_{exi} per unit time.

In these cases, the effect of speed is hidden in the rheological properties of the paste. As already mentioned, if the apex angle of the blade increases, the paste is less compressed, and the shear stress increases. The redistribution of the ratio between the normal stresses σ and the shear stresses τ in favor of shear stresses is associated with the skeletal consolidation of the paste, liquid migration and the rate of shear deformation.

3.4. The Course of the Amount of Extruded Material through the Matrix Depending on the Extrusion Pressure

Figure 10 shows the distribution of moisture in the paste that is in the space between the blade and matrix (control volumes from V_{in1} to V_{in5}) and the extrudate V_{exi} as a function of the extrusion pressure profile P_i . The figures for the individual rotor speeds n_R show how the liquid is distributed between the extrudate and the paste in the wedge for the individual inclinations of the blade angle α_i . This phenomenon is best observed at speeds $n_R = 10 \text{ min}^{-1}$ and blade angle $\alpha_i = 20^\circ$. If the parameters are set in this way in the extruder, the largest difference between the moisture of the extrudate w_{ei} and the moisture of the paste in the wedge w_i occurs. As the angle of inclination of the blade α_i increases, these differences decrease. This is probably due to the fact that at low speeds n_R there is a relatively longer time for the liquid to move in the wedge space and outwards into the extrudate. At the same time, the angle of inclination of the blade α_i again redistributes the ratio between the normal stresses σ and the shear stresses τ in favor of the shear stresses, and thus, it has a positive influence on the paste flow in terms of the rheological properties. The liquid migration is in the opposite direction to the pressure increase.

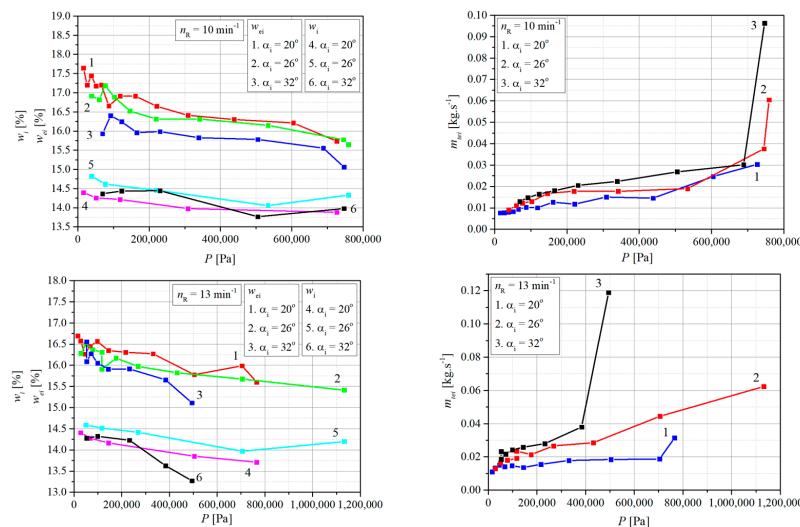


Figure 10. Cont.

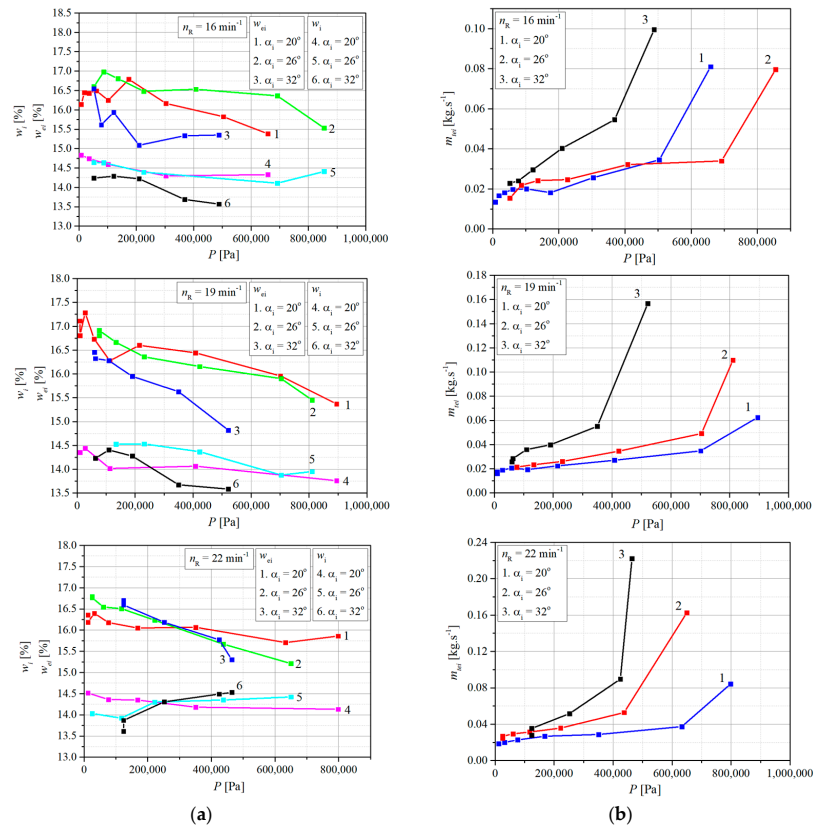


Figure 10. Influence of the extrusion pressure P , blade geometry and rotor speed n_R : (a) on the distribution of the liquid before the matrix w_i , in the extrudate w_{ei} ; (b) on the mass flow of the extrudate through the openings in the matrix m_{tei} .

The course of the mass flow m_{tei} as a function of pressure is also interesting. At the lowest rotor speed $n_R = 10 \text{ min}^{-1}$, the effect of the blade angle α_i is very small. For the angle $\alpha_i = 20^\circ$ the increase in the mass flow of the extrudate m_{tei} is the smallest. This is probably due to the prevailing normal stresses σ . They consolidate the paste and force the liquid to leak through the matrix openings into the extrudate. The consolidated paste has worse flow properties, and it causes the pressure to increase but not the mass flow m_{tei} . By increasing the blade angle α_i , the paste is less consolidated. Due to this, the rheological properties are changed again, and the paste becomes more fluid and the mass flow of the m_{tei} extrudate increases.

Figure 11 shows the interaction of the mass flow of the extrudate through the holes in the matrix m_{tei} and the torque M_{ki} required to drive the rotor. The mass flow m_{tei} is defined in (Figure 7) and depends on the rotor speed n_R . The parameter is the geometry of the blade, represented by the angle between the blade and the surface of the matrix α_i . The effect of rotor speed n_R is hidden in the mass flow of the m_{tei} extrudate.

The torque M_{ki} decreases when increasing the angle α_i . The mass flow of the extrudate m_{tei} has the opposite tendency. For the blade with the apex angle $\alpha_i = 20^\circ$, there is a significant increase of the torque M_{ki} in relation to the increase of the mass flow of the extrudate m_{tei} . This is related to the decomposition of the integral force on the blade F_i in the direction of the normal component N_i and the tangential component T_i (Figure 1). For this blade, the force component N_i predominates, i.e., the normal stress σ , which consolidates the particulate matter, reduces the porosity ε_i and redistributes the moisture of the paste w_i in the wedge gap under the blade. The force N_i pushes the consolidated paste through the holes of the die, but at the same time, it causes a frictional force between the paste and the surface of the matrix. This frictional force contains two basic components.

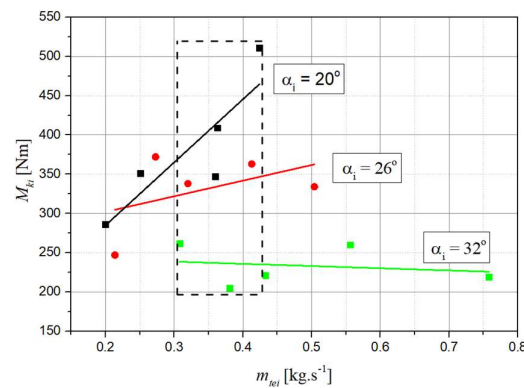


Figure 11. Influence of the mass flow of the extrudate through the holes in the matrix m_{tei} on the torque M_{ki} required to drive the rotor with the blade.

The first force T_{wi} is the friction between the paste and the surface of the matrix. (Figure 1) It is defined by the angle of wall friction for wet powder φ_{wm} [6]. The second one is the result of the internal friction in the paste as it enters a hole in the matrix. The paste is pressed into it by the force N_i but the shear component T_{pi} is the internal friction in the paste. It is defined from the point of view of the mechanics of particulate matter as the angle of internal friction φ_i . According to the rheology, this shear stress is hidden in the apparent viscosity η_z of the paste. The sum of these forces acts on the arm of the radius of the matrix $D_M/2$ and thus the torque M_{ki} is created.

This analysis shows that as α_i increases, the influence of the force N_i decreases and the influence of the force T_i increases.

The main consequence of the redistribution of the ratio between N_i and T_i is the change of the consolidation of the skeleton, i.e., the bulk density of the particulate matter, specifically the density of the paste and the migration of the liquid.

This means that in the marked area (Figure 11) it is possible, while maintaining the mass flow of the extrudate m_{tei} , to change its bulk density and consolidation by changing the geometry of the blade, while other input parameters of the paste need not be changed. The strength of the agglomerates depends on the consolidation of the paste. It follows that their strength can be varied by the geometry of the blade.

4. Conclusions

A model material was used for the experiments. It allowed the testing of a relatively wide range of parameters of the extrusion process. The aim was to find out how the individual parameters, i.e., the rotor speed and the geometry of the blade, affect the behavior of the paste during extrusion.

The scatter of the results is due to the fact that the rheological properties of the paste, made of limestone and sand, are very sensitive to changes in moisture. Therefore, any inhomogeneity causes deviations and impairs the reproducibility of the measurements. The results showed that the geometry of the blade, represented by the angle between the tangents to the matrix and to the blade at the point of contact, affects the pressure distribution in the paste in the wedge gap formed by the surface of the blade and the matrix. The uneven pressure distribution causes the liquid migration in the paste before extrusion. However, the redistribution of moisture in the paste before extrusion, in the wedge gap, and in the extrudate itself is also remarkable.

In basket extruders, the matrix and blades have the shape of curves generally, so that the geometry of the wedge boundary has the shape of a body defined by the areas of these curves. In this case, they are sections from cylindrical surfaces. As a result, the increase of the extrusion pressure is not linear. The smaller the apex angle of the wedge, the more exponential the pressure increase is. On the contrary, as the wedge angle increases, it approaches a linear course. This knowledge is important from the point of view of the consolidation of the

granular skeleton in the direction of increasing pressure. This causes the pores to shrink and the fluid in the paste in the wedge gap to migrate in the opposite direction as the pressure increases. The motion of the liquid in the direction of the widening gap also causes the moisture of the extrudate behind the matrix to change. The least liquid contains extrudate that is extruded close to the narrowest gap. Then, the moisture of the extrudate increases in the opposite direction as the pressure increases under the blade. An interesting finding is the fact that as the distribution of the moisture of the paste in front of the matrix and the extrudate behind the matrix decreases with increasing wedge angle, the distribution of the amount of extruded material increases. This phenomenon can be explained by the fact that the smaller the apex angle, the greater the influence of normal stresses. They, together with shear stresses, consolidate the granular skeleton more intensively.

As a result, the voidage decreases more significantly and the migration of the liquid increases. However, this affects the rheological properties of the paste. This results in the ratio between the output of the extruder and the torque required to drive the rotor with blades to the detriment of the output of the extruder. The results show that the smaller the apex angle, the smaller the amount of extruded material, but the higher the energy requirements for driving the device, i.e., the higher the extrusion pressure, the higher the torque values. Thus, an area has been found where it is possible to influence the magnitude of the torque by changing the geometry of the blade, thus providing a basis for optimizing the quality of the product in terms of energy requirements for the extruder drive. The results also show that the modification of the product quality does not have to be done only by changing the rheological properties of the paste or its composition. This can also be achieved by changing the extrusion pressure. This can be regulated by the inclination of the blade in a device of this type. For pastes that are soft or have a low tendency toward liquid migration, it is possible to use longer blades, creating a wedge gap with a small apex angle. For pastes with a tendency to easily dewater, it is better to use short blades, creating a wedge gap with a larger apex angle.

Author Contributions: Conceptualization, investigation, methodology, writing—original draft preparation, formal analysis, R.F. and P.P.; investigation, M.J., Š.G., M.P. (Marian Peciar) and D.H.; conceptualization, investigation, visualization, resources, M.P. (Michaela Peciarová). All authors have read and agreed to the published version of the manuscript.

Funding: This research was funded by the project of the European Regional Development Fund (313021X329, 313021BXZ1), Slovak Research and Development Agency (APVV-21-0173), and the Ministry of Education, Science, Research and Sport of the Slovak Republic (VEGA 1/0070/22, KEGA 021STU-4/2022, KEGA 003STU-4/2023).

Data Availability Statement: The data presented in this study are available on request from the corresponding author. The data are not publicly available due to the extensive quantity of values.

Conflicts of Interest: The authors declare no conflicts of interest.

Nomenclature

a	[m]	hole spacing
d_M	[m]	diameter of the matrix holes
d_S	[m]	diameter of the pressure sensor membrane
h_M	[m]	matrix thickness
m_{tei}	[kg·s ⁻¹]	mass flow of the extrudate
m_{ei}	[kg]	weight of extrudate
m_{si}	[kg]	weight of the paste under the blade before extrusion in the i^{th} control volume in the dry state
m_{wi}	[kg]	weight of the paste under the blade before extrusion in the i^{th} control volume in the wet state
n_R	[s ⁻¹]	rotor speed
p	[Pa]	pressure
t	[s]	time

w	[-]	absolute moisture of the paste
w_{ei}	[-]	absolute moisture of the extrudate in the i^{th} control volume
w_i	[-]	absolute moisture of the paste under the blade in the i^{th} control volume before extrusion, local moisture of the paste
AIF	[°]	angle of internal friction according to Freeman rheometer FT4
$AIF E$	[°]	angle of internal friction [effective] according to Freeman rheometer FT4
BD	[kg·m ⁻³]	bulk density according to Freeman rheometer FT4
CO	[Pa]	cohesion according to Freeman rheometer FT4
D_M	[m]	inner diameter of the matrix
D_R	[m]	rotor diameter
FF	[-]	flow function according to Freeman rheometer FT4
F_i	[N]	integral force on the blade surface
H_M	[m]	matrix depth
L_i	[m]	blade length
L_{Mi}	[m]	projection of the blade length onto the matrix surface
M_{Ki}	[Nm]	torque
MPS	[Pa]	major principle stress according to Freeman rheometer FT4
N_i	[N]	radial component of integral force, normal force
P	[Pa]	extrusion pressure
P_i	[Pa]	extrusion pressure per i^{th} control volume
P_{cons}	[Pa]	consolidation pressure
R_i	[m]	blade radius
R_{MK}	[m]	arm radius for torque calculation
S	[-]	degree of liquid saturation of pores, saturation
T_i	[N]	tangential component of integral force, shear force
T_{pi}	[N]	shear force in the paste in the shear plane at the entrance to a matrix hole
T_{wi}	[N]	shear force between the paste and the matrix surface
UYS	[Pa]	unconfined yield strength according to Freeman rheometer FT4
V_{ini}	[m ³]	control i^{th} volume between the blade and matrix
V_{exi}	[m ³]	control i^{th} volume containing extrudate
α_i	[°]	the angle between the tangents to the blade and surface of the matrix
ε_i	[-]	voidage, porosity
$\Delta\varepsilon_i$	[-]	porosity difference from sample compaction
$\dot{\gamma}$	[s ⁻¹]	rate of shear strain
η_p	[Pa·s]	plastic viscosity
η_z	[Pa·s]	apparent viscosity
ρ_C	[kg·m ⁻³]	bulk density in the compressibility test
ρ_N	[kg·m ⁻³]	bulk density
ρ_{pi}	[kg·m ⁻³]	bulk density of particulate material or density of a paste after consolidation by extrusion pressure P_i
ρ_S	[kg·m ⁻³]	density
σ	[Pa]	normal stress
σ_C	[Pa]	normal stress in the compressibility test
σ_i	[Pa]	normal stress for the blade inclination at an angle α_i
τ	[Pa]	shear stress
τ_i	[Pa]	shear stress for the blade inclination at an angle α_i
φ_i	[°]	angle of an internal friction
φ_{wm}	[°]	the angle of wall friction between the surface of matrix and paste
Θ	[°]	angle between components of a force
Δt	[s]	time interval
$\Delta\varepsilon_i$	[-]	change of the voidage or porosity
Δw_i	[-]	moisture scattering in the wedge section i
δ	[-]	Kronecker delta
σ	[Pa]	normal stress tensor
τ	[Pa]	shear stress tensor

References

1. Fedá, J. *Mechanics of Particulate Materials—The Principles*; Academia Praha: Prague, Czech Republic, 1982.
2. Novosad, J. *Mechanics of Bulk Materials*; Script, Czech Technical University in Prague: Prague, Czech Republic, 1983. (In Czech)
3. Bird, R.B.; Stewart, W.E.; Lightfoot, E.N. *Transport Phenomena*; John Wiley & Sons: Hoboken, NJ, USA, 2007; ISBN 978-0-470-11539-8.
4. Bendow, J.; Bridgwater, J. *Paste Flow and Extrusion*; Clarendon Press: Oxford, UK, 1993; ISBN 0-19-856338-8.
5. Patel, M.J.; Blackburn, S.; Wilson, D.I. Modelling of paste ram extrusion subject to liquid phase migration and wall friction. *Chem. Eng. Sci.* **2017**, *172*, 487–502. [[CrossRef](#)]
6. Fekete, R.; Peciar, M.; Hanzel, M. Influence of Powder Material Moisture on the Angle of Wall Friction. *Part. Part. Syst. Charact.* **2007**, *24*, 276–283. [[CrossRef](#)]
7. Burbidge, A.S.; Bridgwater, J.; Saracevic, Z. Liquid Migration in Paste Extrusion. *Trans IChemE* **1995**, *73*, 810–816.
8. Liu, H.; Liu, J.; Leu, M.C.; Landers, R.; Huang, T. Factors influencing paste extrusion pressure and liquid content of extrudate in freeze-form extrusion fabrication. *Int. J. Adv. Manuf. Technol.* **2012**, *67*, 899–906. [[CrossRef](#)]
9. Perrot, A.; Rangeard, D.; Mélinge, Y.; Estellé, P.; Lanos, C. Extrusion Criterion for Firm Cement-based Materials. *Appl. Rheol.* **2009**, *19*, 53042-1–53042-7.
10. O'Neill, R.; McCarthy, H.O.; Cunningham, E.; Montufar, E.; Ginebra, M.P.; Wilson, D.I.; Lennon, A.; Dunne, N. Extent and mechanism of phase separation during the extrusion of calcium phosphate pastes. *J. Mater. Sci. Mater. Med.* **2016**, *27*, 29. [[CrossRef](#)]
11. Sherwood, J.D. Liquid–solid relative motion during squeeze flow of pastes. *J. Non-Newton. Fluid Mech.* **2002**, *104*, 1–32. [[CrossRef](#)]
12. Jiang, G.P.; Yang, J.F.; Gao, J.Q. Effect of starch on extrusion behaviour of ceramic pastes. *Mater. Res. Innov.* **2009**, *13*, 119–123. [[CrossRef](#)]
13. Macosko, C.W. *Rheology Principles, Measurements and Applications*; Wiley-VCH: Weinheim, Germany, 1994; ISBN 1-56081-579-5.
14. Liu, H.; Leu, M.C. Liquid phase migration in extrusion of aqueous alumina paste for freeze-form extrusion fabrication. *Int. J. Mod. Phys. B* **2009**, *23*, 1861–1866. [[CrossRef](#)]
15. Fekete, R. Influence of the Rotor Pressure Effect on the Extrusion Process. Ph.D. Thesis, Slovak University of Technology in Bratislava, Bratislava, Slovakia, 2002. (In Slovak).
16. Maderová, K. Liquid Phase Migration During Paste Extrusion. Ph.D. Thesis, Slovak University of Technology in Bratislava, Bratislava, Slovakia, 2012. (In Slovak).
17. Poláková, K. Shear Strength of Wet Particulate Materials. Ph.D. Thesis, Slovak University of Technology in Bratislava, Bratislava, Slovakia, 2012. (In Slovak).
18. Vadaga, A.K.; Gudla, S.S.; Nareboina, G.S.K.; Gubbala, H.; Golla, B. Comprehensive Review of Modern Techniques of Granulation in Pharmaceutical Solid Dosage Forms. *Intell. Pharm.* **2024**, *in press*. [[CrossRef](#)]
19. Bandari, S.; Nyavanandi, D.; Kallakunta, V.R.; Janga, K.Y.; Sarabu, S.; Butreddy, A.; Repka, M.A. Continuous twin screw granulation—An advanced alternative granulation technology for use in the pharmaceutical industry. *Int. J. Pharm.* **2020**, *550*, 119215. [[CrossRef](#)] [[PubMed](#)]
20. Shanmugam, S. Granulation techniques and technologies: Recent progresses. *BioImpacts* **2015**, *5*, 55–63. [[CrossRef](#)] [[PubMed](#)]
21. Dhenge, R.M.; Cartwright, J.J.; Hounslow, M.J.; Salman, A.D. Twin screw wet granulation: Effects of properties of granulation liquid. *Powder Technol.* **2012**, *229*, 126–136. [[CrossRef](#)]
22. Zukowski, S.R.; Kodam, M.; Khurana, S.; Taylor, J.; Frishcosy, M.; Hercamp, J.; Snedeker, J.; Williams, E. Performance comparison of dome and basket extrusion granulation. *Chem. Eng. Res. Des.* **2020**, *160*, 190–198. [[CrossRef](#)]
23. Horrobin, D.J.; Nedderman, R.M. Extrusion Pressure Estimation in Axisymmetric Paste Extrusion. *KONA* **1999**, *17*, 122–129. [[CrossRef](#)]
24. Zhang, M.; Mascia, S.; Rough, S.L.; Ward, R.; Seiler, C.; Wilson, D.I. A novel lab-scale screen extruder for studying extrusion-spheronisation. *Int. J. Pharm.* **2013**, *455*, 285–297. [[CrossRef](#)] [[PubMed](#)]
25. Zhang, M.; Rough, S.L.; Ward, R.; Seiler, C.; Wilson, D.I. A comparison of ram extrusion by single-holed and multi-holed dies for extrusion-spheronisation of microcrystalline-based pastes. *Int. J. Pharm.* **2011**, *416*, 210–222. [[CrossRef](#)]
26. Russell, B.D.; Lasenby, J.; Blackburn, S.; Wilson, D.I. Monitoring Structural Aspects of Pastes Undergoing Continuous Extrusion Using Signal Processing of Pressure Data. *Chem. Eng. Res. Des.* **2004**, *82*, 770–783. [[CrossRef](#)]
27. Rough, S.; Bridgwater, J.; Wilson, D. Effects of liquid phase migration on extrusion of microcrystalline cellulose pastes. *Int. J. Pharm.* **2000**, *204*, 117–126. [[CrossRef](#)]
28. Rumpf, H. Zur Theorie der Zugfestigkeit von Agglomeraten bei Kraftübertragung an Kontaktpunkten. *Chem. Ing. Tech.* **1970**, *42*, 538–540. (In German) [[CrossRef](#)]
29. Mascia, S.; Seiler, C.; Fitzpatrick, S.; Wilson, D.I. Extrusion-spheronisation of microcrystalline cellulose pastes using a non-aqueous liquid binder. *Int. J. Pharm.* **2010**, *389*, 1–9. [[CrossRef](#)] [[PubMed](#)]
30. Dreu, R.; Širca, J.; Pintye-Hodi, K.; Burjan, T.; Planinšek, O.; Srčič, S. Physicochemical properties of granulating liquids and their influence on microcrystalline cellulose pellets obtained by extrusion-spheronisation technology. *Int. J. Pharm.* **2005**, *291*, 99–111. [[CrossRef](#)]
31. Domanti, A.T.J.; Horrobin, D.J.; Bridgwater, J. An investigation of fracture criteria for predicting surface fracture in paste extrusion. *Int. J. Mech. Sci.* **2002**, *44*, 1381–1410. [[CrossRef](#)]

32. A Report of the EFCE Working Party on the Mechanics of Particulate Solids. In *Standard Shear Testing Techniques for Particulate Solids Using the Jenike Shear Cell*; The Institute of Chemical Engineers EFCE: Rugby, UK, 1989; ISBN 0852952325.
33. Rough, S.L.; Wilson, D.I.; Bridgwater, J. A Model Describing Liquid Phase Migration within an Extruding Microcrystalline Cellulose Paste. *Chem. Eng. Res. Des.* **2002**, *80*, 701–714. [[CrossRef](#)]
34. Mason, M.S.; Huang, T.; Landers, R.G.; Leu, M.C.; Hilmas, G.E. Aqueous-based extrusion of high solids loading ceramic pastes: Process modeling and control. *J. Mater. Process. Technol.* **2009**, *209*, 2946–2957. [[CrossRef](#)]
35. Bryan, M.P.; Rough, S.L.; Wilson, D.I. Investigation of static zones and wall slip through sequential ram extrusion of contrasting micro-crystalline cellulose-based pastes. *J. Non-Newton Fluid Mech.* **2015**, *220*, 57–68. [[CrossRef](#)]
36. Roussel, N.; Lanos, C.; Mélinge, Y. Induced heterogeneity in saturated flowing granular media. *Powder Technol.* **2003**, *138*, 68–72. [[CrossRef](#)]
37. Daniels, K. Force Chains in a Photoelastic Granular Material. 2017. Available online: https://danielslab.physics.ncsu.edu/dcp_0866 (accessed on 17 May 2024).
38. Roussel, N.; Lanos, C. Particle Fluid Separation in Shear Flow of Dense Suspensions: Experimental Measurements on Squeezed Clay Pastes. *Appl. Rheol.* **2004**, *14*, 256–265. [[CrossRef](#)]

Disclaimer/Publisher’s Note: The statements, opinions and data contained in all publications are solely those of the individual author(s) and contributor(s) and not of MDPI and/or the editor(s). MDPI and/or the editor(s) disclaim responsibility for any injury to people or property resulting from any ideas, methods, instructions or products referred to in the content.